IEEE SIGNAL PROCESSING SOCIETY
INTERNATIONAL SYMPOSIUM ON TIME-FREQUENCY AND TIME-SCALE ANALYSIS,
PARIS, JUNE 18-21 1996.

DIRECTIONAL IMAGE COMPRESSION WITH BRUSHLETS

François G. Meyer, and Ronald R. Coifman

Department of Mathematics, Yale University, 12 Hillhouse ave, New Haven CT, 06520, USA.
e-mail: meyer@noodle.med.yale.edu

ABSTRACT

We construct a new adaptive basis that provide precise frequency localization and good spatial localization. We develop a compression algorithm that exploits this basis to obtain the most economical representation of the image in terms of textured patterns with different orientations, frequencies, sizes, and positions. The technique directly works in the Fourier domain and has potential applications for highly textured images.

1. INTRODUCTION

Edges and textures in an image can exist at all possible locations, orientations, and scales. The ability to efficiently analyze and describe textured patterns is thus of fundamental importance for image analysis and image compression. Wavelets provide an octave based decomposition of the Fourier plane with a poor angular resolution. Wavelet packets make it possible to adaptively construct an optimal tilling of the Fourier plane, and they have been used for image compression [1]. However a wavelet is always associated with two peaks in frequency that does not allow to selectively localize a unique frequency. We propose to adaptively segment the Fourier plane to obtain the most concise and precise representation of the image in terms of oriented textures with all possible directions, frequencies, and locations. To achieve this we have constructed a new family of orthogonal functions that we call *brushlets*.

This paper is organized as follows. In the next section we review the construction of smooth localized orthonormal exponential basis. In section 3 we describe the new brushlet basis. In section 4 we describe the image compression algorithm based on a brushlet expansion of the image. Results of experiments are presented in Section 5.

2. LOCAL TRIGONOMETRIC BASES

First we review the construction of smooth localized orthonormal exponential basis [2, 3]. These functions are exponentials with good localization in both position and Fourier space. We consider a cover $\mathbb{R} = \bigcup_{n=-\infty}^{n=+\infty} [a_n, a_{n+1}[$. We write $l_n = a_{n+1} - a_n$, and $c_n = (a_n + a_{n+1})/2$. Around each a_n we define a neighborhood of radius ε. Let r be a ramp function such that

$$r(t) = \begin{cases} 0 & \text{if} \quad t \leq -\varepsilon \\ 1 & \text{if} \quad t \geq \varepsilon \end{cases} \tag{1}$$

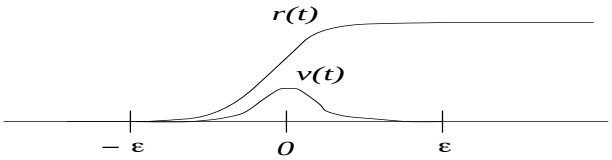

Figure 1: Ramp function r, and bump function v.

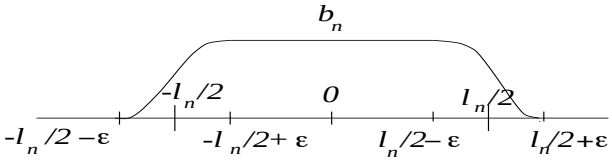

Figure 2: Windowing function b_n.

and

$$r^2(t) + r^2(-t) = 1, \qquad \forall t \in \mathbb{R} \tag{2}$$

Let v be the bump function supported on $[-\varepsilon, \varepsilon]$ (see Fig. 1)

$$v(t) = r(t)r(-t) \tag{3}$$

Let b_n be the windowing function supported on $[-l_n/2 - \varepsilon, l_n/2 + \varepsilon]$ (see Fig. 2)

$$\begin{array}{rcll} b_n(t) & = & r^2(t + l_n/2) & \text{if} \quad t \in [-l_n/2 - \varepsilon, -l_n/2 + \varepsilon] \\ & = & 1 & \text{if} \quad t \in [-l_n/2 + \varepsilon, l_n/2 - \varepsilon] \\ & = & r^2(l_n/2 - t) & \text{if} \quad t \in [l_n/2 - \varepsilon, l_n/2 + \varepsilon] \end{array} \tag{4}$$

We consider the collection of exponential functions $e_{j,n} = e^{-2i\pi j(\frac{x - a_n}{l_n})}$, and we construct a basis of smooth localized orthonormal exponential functions $u_{j,n}$. Each $u_{j,n}$ is supported on $[a_n - \varepsilon, a_{n+1} + \varepsilon]$ and is given by [3]

$$\begin{array}{rcl} u_{j,n}(x) & = & b_n(x - c_n)e_{j,n}(x) \\ & + & v(x - a_n)e_{j,n}(2a_n - x) \\ & - & v(x - a_{n+1})e_{j,n}(2a_{n+1} - x) \end{array} \tag{5}$$

We have the following result [2, 3]

Theorem 1 [2, 3] *The collection* $\{u_{j,n}\ j, n \in \mathbb{Z}\}$ *is an orthonormal basis for* $L^2(\mathbb{R})$

We note that this basis uses exponentials, other smooth local bases that use sines, or cosines only can be also constructed [2, 4].

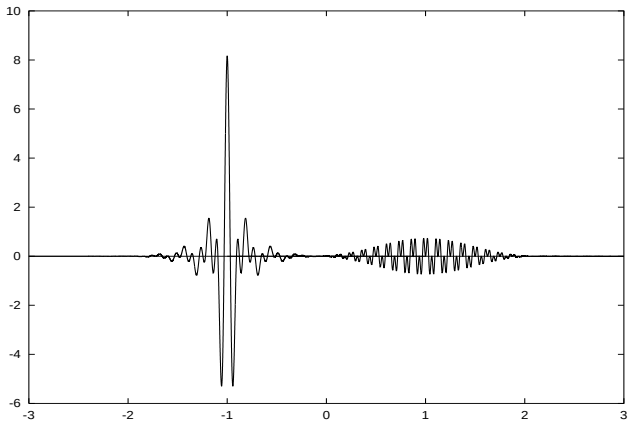

Figure 3: Graph of the real part of $w_{j,n}$. On the left is the principal part of the brushlet: a windowed exponential. On the right is the part necessary to obtain perfect localization in Fourier space. In the two-dimensional case, with tensor products of brushlets, this part can be neglected.

3. ORTHONORMAL BRUSHLET BASES

3.1. One-dimensional case

We now construct the orthonormal brushlet bases. Let $w_{j,n}$ be the inverse Fourier transform of $u_{j,n}$. Since the Fourier transform is a unitary operator, we have

Lemma 1 *$\{w_{j,n}, j, n \in \mathbb{Z}\}$ is an orthonormal basis for $L^2(\mathbb{R})$*

We call $\{w_{j,n}\}$ the orthormonal brushlet basis. We have

$$w_{j,n}(x) = e^{2i\pi c_n x}\left\{(-1)^j \widehat{b}(x-\frac{j}{l}) - 2i\, sin(\pi l\, x)\hat{v}(x+\frac{j}{l})\right\} \tag{6}$$

The function $w_{j,n}$ is composed of two terms, localized around j/l, and around $-j/l$, that are oscillating with the frequency $c_n = (a_n + a_{n+1})/2$. The first term is an exponential multiplied by the window $\widehat{b}_n$. Since $|\hat{v}(x)| \leq \varepsilon$, the second term can be made as small as possible. However, when ε tends to zero the first term is not localized anymore. There is a tradeoff between the localization of $\widehat{b}_n$ and the magnitude of the second term. We choose ε such that the brushlet function is mainly localized around j/l_n. Figure 3 shows the graph of the real part of $w_{j,n}$ for a particular choice of r. If we impose $\widehat{b}_n$ to be positive, then we need to relax condition (2). In this case we can construct *biorthogonal* bases, as explained in [5].

3.2. Two-dimensional case

In the two-dimensional case we define two partitions of $\mathbb{R}$, $\bigcup_{n=-\infty}^{n=+\infty}[a_n, a_{n+1}[$, and $\bigcup_{m=-\infty}^{m=+\infty}[b_m, b_{m+1}[$. We write $l_n = a_{n+1} - a_n$, and $h_m = b_{m+1} - b_m$. We then consider the tilling obtained by the tensor products $[a_n, a_{n+1}[\otimes[b_m, b_{m+1}[$. We consider the separable tensor products of bases $w_{j,n}$, and $w_{k,m}$. We have

Lemma 2 *The sequence $\{w_{j,n} \otimes w_{k,m}\}$ is an orthonormal basis for $L^2(\mathbb{R}^2)$*

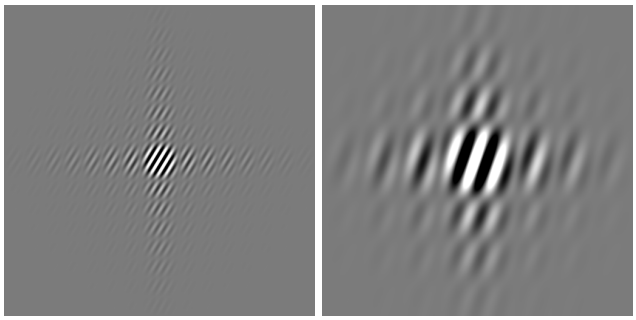
Figure 4: Two dimensional brushlet basis functions $\{w_{j,n} \otimes w_{k,m}\}$ A good spatial resolution corresponds to a $\hat{b}$ with a small support, and is thus associated with a poor frequency resolution as shown on the left. A good frequency resolution corresponds to a b with a small support, and is thus associated with a poor spatial resolution as shown on the right.

The tensor product $w_{j,n}(x) \otimes w_{k,m}(y)$ is an oriented pattern oscillating with the frequency $((a_n + a_{n+1})/2, (b_m + b_{m+1})/2)$ and localized at $(j/l_n, k/h_m)$, as shown in Fig. 4. The size of the pattern is inversely proportional to the size of the analyzing window: $h \times l$ in the Fourier space. We note that the decomposition achieved by wavelet packets does not permit us to localize a unique frequency, for instance in the positive part of the Fourier space. Indeed two symmetric windows are always associated with a wavelet. As a result a wavelet packet expansion will require many more coefficients to describe a pattern with an arbitrary orientation; whereas the same pattern can be coded with a single brushlet coefficient.

3.3. Adaptive tilling of the Fourier plane

As explained in [2, 3] we can adaptively select the size and location of the windows $[a_n, a_{n+1}[\times[b_m, b_{m+1}[$ with the best basis algorithm. We consider only tillings that can be generated from separable bases. We divide the Fourier plane into four sub-squares, and we consider the brushlet basis associated with this tilling. We then further decompose each square into four sub-squares, and consider the brushlet basis associated with this finer tilling. By applying this decomposition recursively we obtain a homogeneous quadtree-structured decomposition. For each subblock, or node of the quadtree, we calculate the set of coefficients associated with the brushlets living on the subblock. If we associate a cost for each node of the tree, based on the set of coefficients, then we can find an optimal segmentation of the Fourier space. Using a divide and conquer algorithm, group of four connected nodes are pruned if their total cost is greater than the cost of their father. The process is recursively applied from the bottom to the top of the quadtree, and a global optimal tree is then found.

3.4. Image compression

We have developed a coding algorithm that exploits a brushlet expansion of the image.

3.4.1. Adaptive brushlet decomposition

The Fourier transform $\hat{f}$ of the image f is computed using a FFT. $\hat{f}$ is hermitian-symmetric, therefore we only retain the upper half of the Fourier plane $\{(\nu,\xi),\xi \geq 0\}$ for coding. We divide the upper half into two quadrants. For each quadrant the brushlet coefficients are calculated at different resolutions. Instead of calculating the inner product of $\hat{f}$ with $u_{j,n} \times u_{k,m}$ we fold the image around the horizontal and vertical lines associated with the tilling [3]. We then calculate inside each block the 2-D FFT of the folded block, and obtain the brushlet coefficients. Finally, we estimate the optimal tilling using the brushlet bases at different resolution. Each block associated with the segmentation corresponds to a set of brushlet coefficients. These coefficients describe the intensity of one single "brush stroke" at different locations in the image, as illustrated in Fig. 6. This "brush stroke" has a particular frequency, orientation, and size, that are given by the position of the block, and its size.

3.4.2. Quantization and zig-zag scanning of the coefficients

The brushlet coefficients are quantized with uniform quantizers. In order to exploit the correlation between brushlet coefficients in different subbands, we order all the brushlet coefficients associated with the same spatial location. The coefficients are ordered by increasing frequency order by scanning the quadrant with a zig-zag pattern as shown in Fig. 5. Since the magnitude of the terms in a zig-zag sequence decreases with an exponential decay, we encode a terminating symbol after the last non-zero coefficient to indicate that the remaining coefficients are zeros. This represents a zero-tree like extension of the algorithm proposed in [6].

3.4.3. Entropy coding

After zig-zag ordering, the coefficients are coded using variable length coding. The alphabet that describes the variable length encoding is entropy coded with an adaptive arithmetic coder. The first term of a zig-zag scan corresponds to a DC coefficient. The DC coefficients of adjacent spatial locations are still correlated, and are therefore differentially encoded.

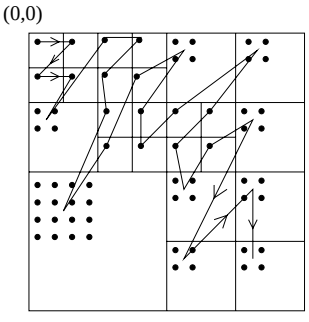

Figure 5: We order all the brushlet coefficients associated with the same spatial location using a zigzag pattern.

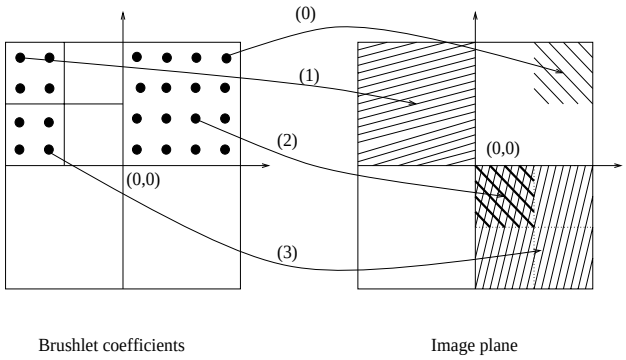

Figure 6: Each pixel in a brushlet subblock corresponds to a subblock in the image plane. Conversely, each pixel in the image is decomposed into different brushlets. A good spatial resolution is associated with a poor frequency resolution as in (2). A good frequency resolution is associated with a poor spatial resolution as in (1) and (3). The best basis algorithm finds the optimal compromise between these two constraints with respect to the content of the image.

We have implemented the coder and decoder, and an actual bit stream was created for each experiment. We present the results of the algorithm using two test images that are difficult to compress: 512x512 "Barbara", and 512x512 "Mandrill". The performance of the algorithm are summarized in Table 1, and results for compression ratios of 82:1 and 81:1 are shown in Fig. 3. Figure 3 shows the optimal tilling of the two quadrants of the upper half of the Fourier plane. We note that the segmentation is not symmetric, reflecting some oriented textures in the images. We also note that even at a compression ratio of 81:1 the mandrill still keeps its high frequency features such as the whiskers.

4. REFERENCES

[1] K. Ramchandran and M. Vetterli. Best wavelet packet bases in a rate-distortion sense. *IEEE Trans. on Image Processing*, pages pp 160–175, April 1993.

[2] R.R. Coifman and Y. Meyer. Remarques sur l'analyse de fourier à fenêtre. *C.R. Acad. Sci. Paris I*, pages pp. 259–261, 1991.

[3] M.V. Wickerhauser. *Adapted Wavelet Analysis from Theory to Software*. A.K. Peters, 1995.

[4] I. Daubechies, S. Jaffard, and J.L. Journé. A simple wilson orthonormal basis with exponential decay. *SIAM J. Math. Anal.*, 22:554–572, 1991.

[5] F.G. Meyer and R.R. Coifman. Biorthogonal brushlet bases for directional image compression. In *12th International Conference on Analysis and Optimization of Systems,Images, Wavelets and PDE's, 26-28 juin 1996, Paris, France*, page to appear. Springer Verlag, 1996.

[6] J.M. Shapiro. Embedded image coding using zerotrees of wavelet coefficients. *IEEE Trans. on Signal Processing*, pages 3445–3462, Dec. 1993.

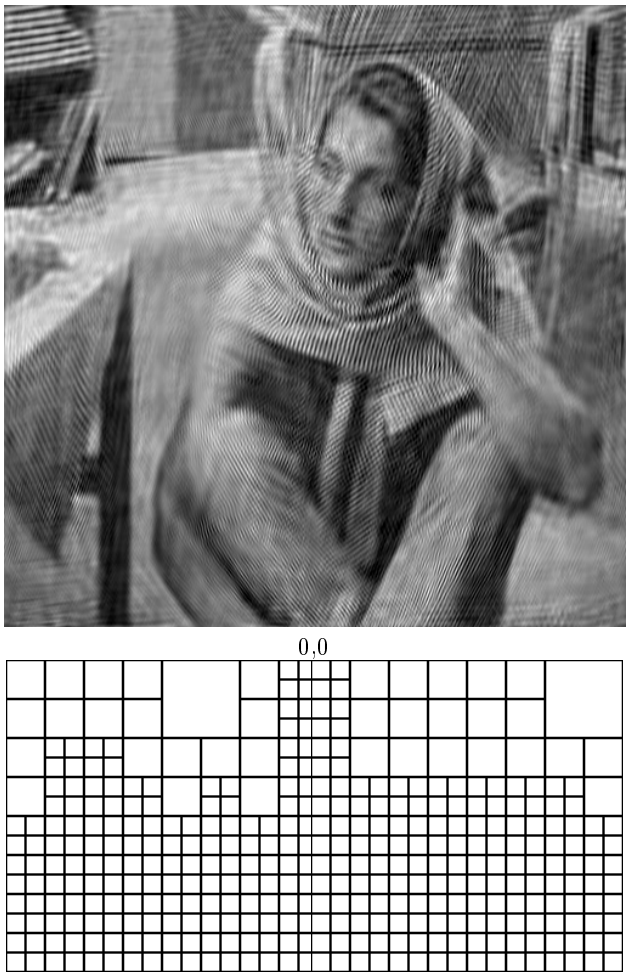

Figure 7: (a) Barbara, compression 82:1. (b) Optimal tilling of the upper half of the Fourier plane; the horizontal axis point toward the right, and the vertical axis points upwards.

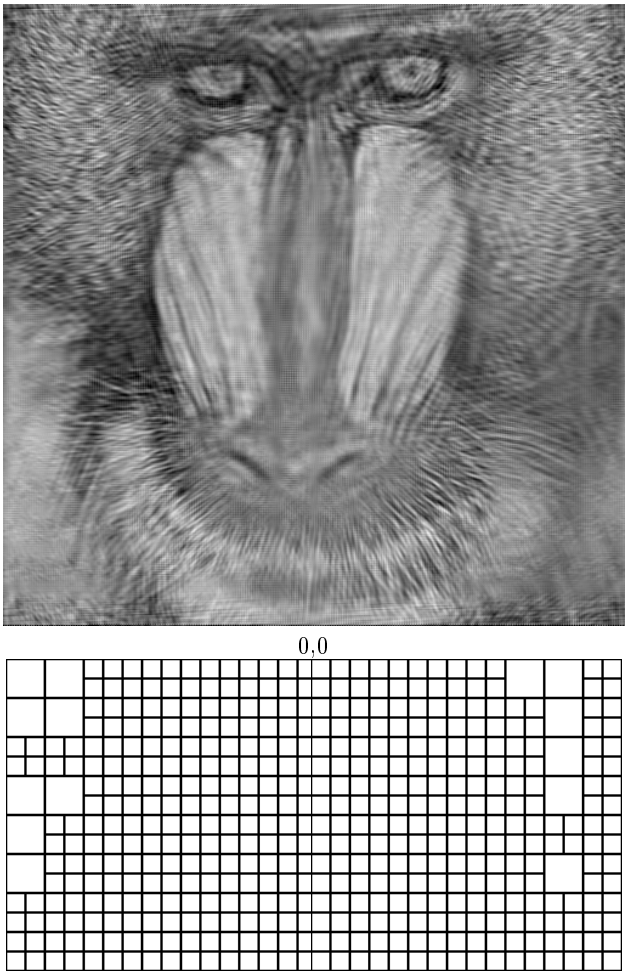

Figure 8: (a) Mandrill, compression 81:1. (b) Optimal tilling of the Fourier plane for Mandrill.

	Barbara
Compression	PSNR (dB)
8:1	35.30
16:1	30.86
32:1	25.15
67:1	23.47
82:1	23.08
135:1	22.06
334:1	20.31

Table 1: Coding results for 8bpp. 512x512 Barbara

	Mandrill
Compression	PSNR (dB)
8:1	28.28
15:1	25.34
30:1	23.14
58:1	21.76
81:1	21.26
121:1	20.71
206:1	20.19

Table 2: Coding results for 8bpp. 512x512 Mandrill